THE USE OF ADVANCED SPACEBORNE THERMAL EMISSION AND REFLECTION RADIOMETER IMAGERY IN SOIL FERTILITY INVESTIGATION OF A FARMLAND IN ILE-IFE NIGERIA

Francis Omotayo Adekayode, Doctor
Department of Crop, Soil and Pest Management,
Federal University of Technology, Akure, Nigeria
Abdul-Rahman Adegbite, Doctoral Candidate
Rufus Olakunle Oladosu, Doctor
African Regional Centre for Space Science and Technology Education
(Arcsste-E), OAU Campus, Ile-Ife, Nigeria

Abstract

The Advanced Spaceborne Thermal Emission and Reflection Radiometer (ASTER) image of a 350 hectare farmland in Ile-Ife ($7^0$33'N, $4^0$33'E), Nigeria was processed to generate the contour and slope maps in a soil fertility investigation in 2012. The image Focal Statistics were generated using the Spatial Analyst/ Neighborhood/Focal Statistics Tools in ArcMap and the contour map generated at an interval of 5 m using the Spatial Analyst/ Surface/ Contour Tools while the slope map generated by using the Spatial Analyst/ Surface/ Slope Tools. Four slope classes of 0 to 2%, 2 to 4%, 4 to 6% and 6 to 8% were generated and soil samples taken from five sampling locations in each slope class for laboratory analyses for nitrogen, phosphorus, potassium and organic matter content. Surface interpolation for the generation of the spatial distribution of each of the nutrient concentrations was carried out with the 3D Analyst / Raster Interpolation / Kriging Tools while the overlay operation to generate the fertility classes were carried with the 3D/Raster Math Tools. Four fertility classes of low, medium, marginally good and good were mapped. The soil nutrient level of the greater part of the farmland was of medium to marginally good productivity classes while the percentage areas covered by low, medium, marginally good and good fertility classes were 11, 41, 39 and 9 % respectively.

Keywords: ASTER imagery, soil nutrient concentration, fertility classes

Introduction

The quality of the soil that enabled it to provide essential chemical elements in quantities and proportions for the growth of specific crops had been defined as soil fertility (Juo and Franzluebbers, 2003). Soil fertility depended on such factors as texture, structure, soils supply of water, soil temperature and the chemical composition with its content of plant nutrients and the activities of soil organisms (Havlin et al., 2009).

The potentiality of the soil which could indicate sufficient nutrient availability and deficiencies could be determined by soil test through composite soil sampling from several locations for laboratory analyses and an eventual production of a reference map that would record the location of field samples and the spatial representation of nutrient concentration for logical interpretation (Carrow, 1995; Malindo, 2008).

Soil sampling methods for laboratory analysis could be carried out both by the conventional and geospatial techniques. The conventional technique entailed dividing field into uniform areas of soil association or soil series based on soil colour, topography and past soil management practices with each series sampled separately by taking subsamples randomly in each area (Franzen et al., 1998). The geospatial technique consisting of grid cell sampling, grid centre sampling and the directed soil sampling were explained in previous report (Mallarino and Wittry. 2004; Dinkins, 2008). In the grid cell sampling method, the computer generated grid would be superimposed on the farm perimeter to determine sample locations and a number of subsamples taken randomly from which in each cell, soils were bulked to form one sample. The grid centre method was also based on grid but a DGPS was used to navigate to the centre point of the grid and soil samples taken from a specified radius around the centre point to form the cell sample. The directed soil sampling method was not based on grid but rather on spatial patterns defined by prior knowledge of field variability defined by such factor as slope.

The report of several other soil fertility investigations with the use of remote sensing techniques were contained in previous investigation (Singh and Subramanian, 1982; Cook et al., 1996; Ben-Dor and Parkin, 2002; Chabrillat et al., 2002; Zribi et al., 2011; Li et al., 2012). The use of soil colour as a parameter for soil fertility investigation was reported by Kumar et al. (2013) by using the minimum classification algorithm of landsat image of Vellore District, India while Luo et al. (2008) mapped soil organic matter using airborne hyperspectral reflective remote sensing methodology.

The objectives of this study were to use remotely sensed Advanced Spaceborne Thermal Emission and Reflection Radiometer (ASTER) image to produce the contour and slope maps of a farmland and collect soil samples across slope for the determination of nitrogen, phosphorus, potassium concentration and the organic matter content for the production of soil fertility map.

Materials and Method:
The flow chart for the methodology adopted in sequence is shown in Figure1.

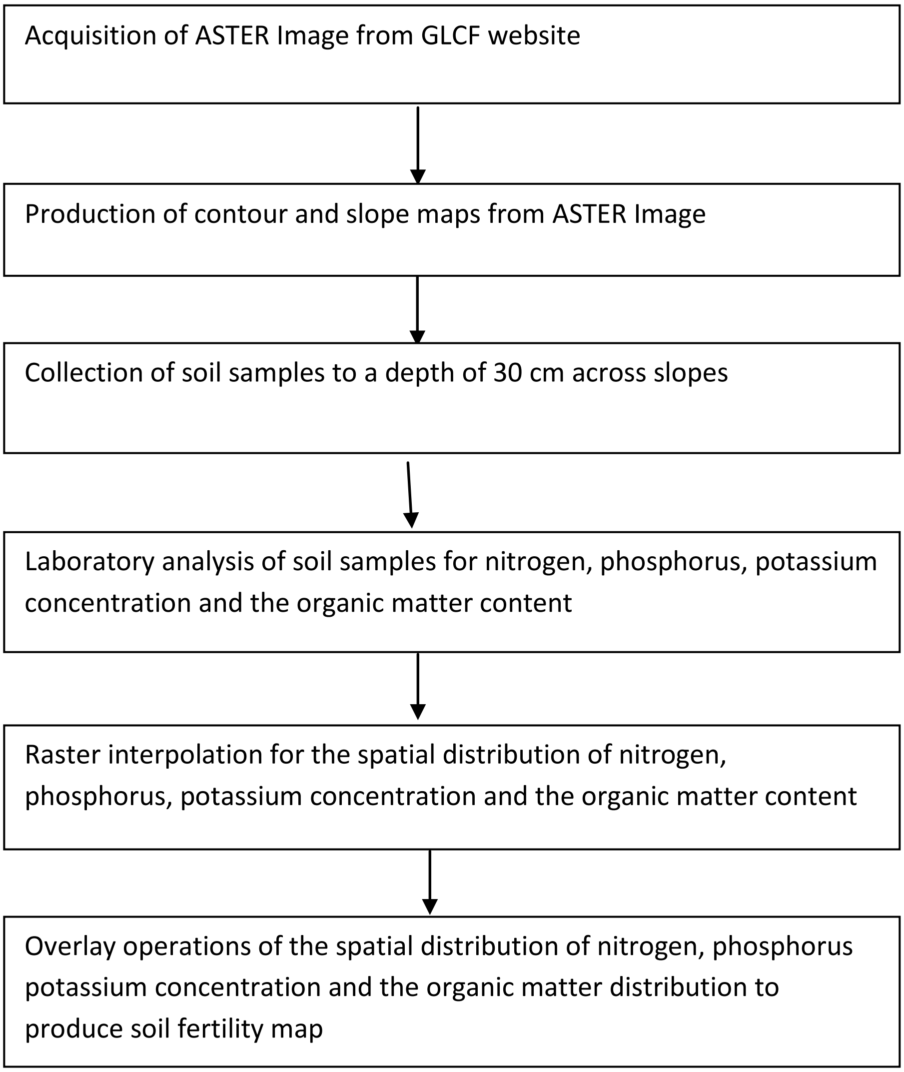

Figure 1: The Flow Chart of the sequence of fertility map from ASTER generated slope map

Generation of contour and slope maps from Advanced Spaceborne Thermal Emission and Reflection Radiometer (ASTER) image

The ASTER image of Ile-Ife at 90 m resolution was downloaded from the Global Land Cover Facility/ASTER imagery site (USGS and Japan

ASTER Programme, 2003). The downloaded image which was in geographic coordinate systems was transformed to the projected coordinate systems of WGS 1984 UTM Zone 31N using the sequential procedure of Data frame/Properties/Predefined Tools in ArcMap. The polygonized boundary of the project site was superimposed on the Ile-Ife ASTER image and the boundary extracted out using the Spatial Analyst/ Extraction by Mask Tools in ArcMap.

The image focal statistics were generated using Spatial Analyst /Neighbourhood/ Focal Statistics Tools in ArcMap while the contour generated at an interval of 5 m with the Spatial Analyst/Surface/ Contour Tools. The slope map was produced using the Spatial Analyst/Surface/ Slope Tools.

Soil sampling and laboratory analysis

Soil samples to a depth of 30 cm from seven locations in each slope were taken for laboratory analysis. Soil samples were air-dried and sieved through a 2 mm sieve and analysed for nitrogen, phosphorus, potassium and organic matter content following the laboratory procedures described by Carter (1993). Organic carbon was determined by oxidising soil sample with dichromate solution and later titrated with ferrous sulphate solution. The total nitrogen was determined using micro-kjeldahl method and the available phosphorus determined by the Bray P-1 method. The exchangeable cations were extracted by leaching 5 g of soil with 50 ml ammonium acetate at pH 7 and the potassium in the leachate determined with a flame spectrophotometer.

Interpolation technique for spatial distribution of nitrogen, phosphors, potassium and the organic matter content and overlay operations for production of soil fertility map

The spatial distribution of nitrogen, phosphors, potassium concentration and the organic matter content was carried out separately for each element with the 3D Analyst/Raster Interpolation/Kriging Tools while the overlay operations to generate the soil fertility map was carried out using the 3D Analyst/Raster Math/Plus Tools in ArcMap.

Result:

Figure 1 shows the contour map at an interval of 5 meters with the lowest and highest elevation of 250 m and 275 m above sea level respectively. The contour map was generated from the ASTER image downloaded from the Global Land Cover Facility (GLCF) site. Figure 2 shows the slope map generated from the contour map with the sampling points for soil sample collections. The soil samples were collected across the slope categories to a depth of 30 cm for laboratory analysis for nitrogen, phosphorus, potassium and organic matter content. The slope was categorized into 0 to 2%, 2 to 4%, 4 to 6% and 6 to 8%.

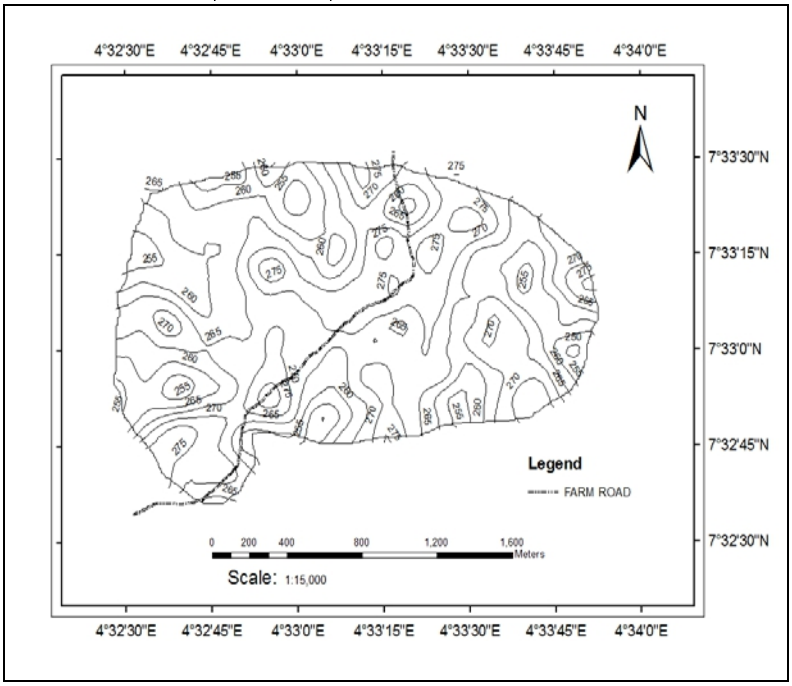

Figure 1: The contour map at an interval of 5 meters and elevation between 250 and 275 m above sea level

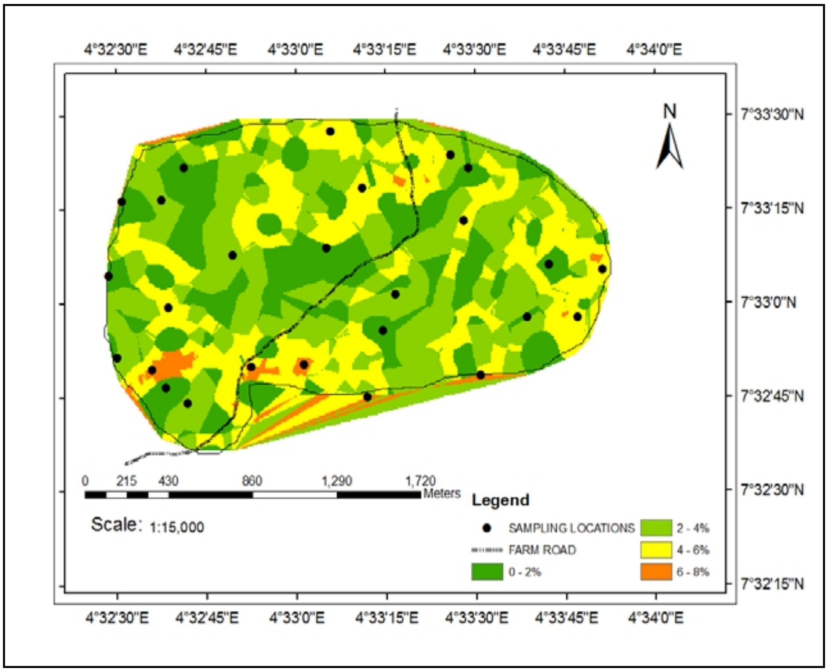

Figure 2: The slope map with soil sampling points across the slope categories

Table 1 shows the nutrient concentration of nitrogen, phosphorus, potassium and organic matter across the various slope categories. The mean values of nitrogen, phosphorus, potassium and organic matter on slope 0 to 2%, 2 to 4%, 4 to 6% and 6 to 8% showed nitrogen concentration as 0.28%, 0.23%, 0.18% and 0.14% respectively; phosphorus as 15.28 ppm, 13.90 ppm, 12.75 ppm and 11.47 ppm respectively; potassium as 0.34 cmol/kg, 0.29 cmol/kg, 0.25 cmol/kg and 0.23 cmol/kg respectively and organic matter as 3.79%, 3.20%, 3.10% and 2.64% respectively.

Table 1: The values of nitrogen, phosphorus, potassium and organic matter content at five locations on each slope in the farmland

Slope	Easting	Northing	N (%)	P (mg/kg)	K (cmol/kg)	OM (%)
0-2%	670432.00	835519.00	0.22	14.46	0.34	3.76
0-2%	671889.00	835519.00	0.29	14.58	0.33	4.07
0-2%	670343.00	834443.00	0.27	14.52	0.36	4.38
0-2%	671452.00	834723.00	0.32	15.18	0.36	3.31
0-2%	672304.00	835048.00	0.31	17.64	0.32	3.41
2-4%	670320.00	835362.00	0.16	14.52	0.28	3.02
2-4%	671800.00	835586.00	0.22	14.58	0.29	3.21
2-4%	671519.00	834903.00	0.25	14.46	0.26	3.34
2-4%	670455.00	834365.00	0.27	12.03	0.32	3.24
2-4%	672192.00	834791.00	0.23	13.92	0.30	3.21
4-6%	671183.00	835698.00	0.14	12.03	0.30	2.86
4-6%	670354.00	834835.00	0.20	13.62	0.24	2.97
4-6%	671867.00	835261.00	0.16	12.96	0.23	2.90
4-6%	672450.00	834791.00	0.20	13.26	0.22	3.34
4-6%	671116.00	834342.00	0.22	11.88	0.24	3.41
6-8%	670270.00	834529.00	0.14	11.67	0.19	2.16
6-8%	670780.00	834544.00	0.13	11.82	0.21	2.21
6-8%	671049.00	834555.00	0.16	11.58	0.20	3.00
6-8%	671953.00	834503.00	0.11	11.04	0.23	2.79
6-8%	671376.00	834397.00	0.14	11.22	0.32	3.03

Figures 3, 4, 5 and 6 show the spatial distribution of nitrogen, phosphorus, potassium and organic matter content respectively and categorised into low, medium, moderately high and high while Figure 7 show the soil fertility map categorized into low, medium, marginally good and good fertility classes and Figure 8 show the percentage area coverage of 11, 41, 39 and 9% of low, medium, marginally good and good fertility classes of the farmland.

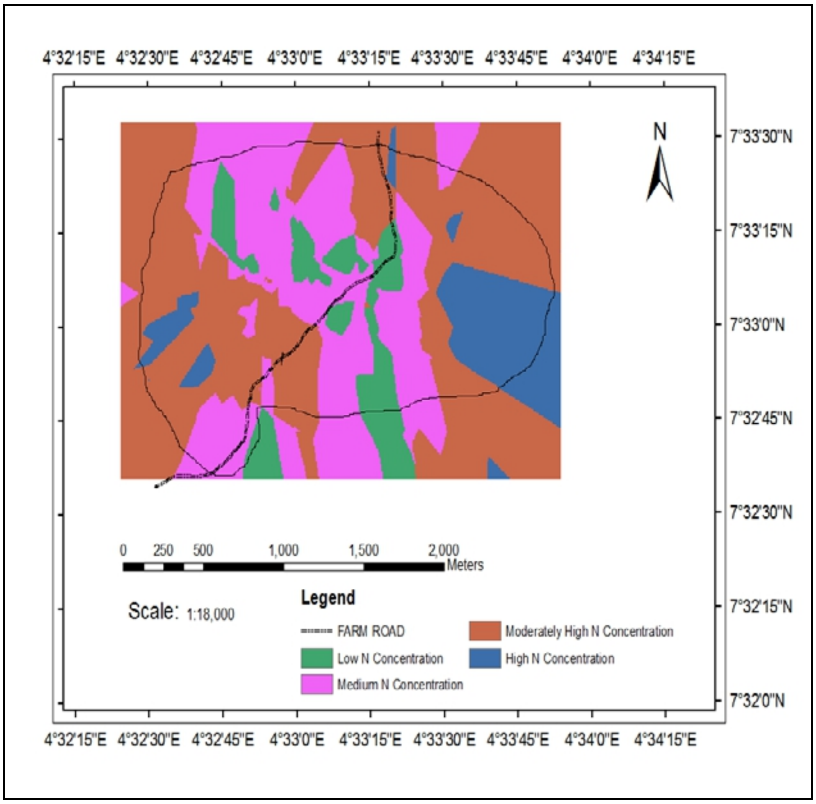

Figure 3: Spatial distribution of nitrogen concentraion

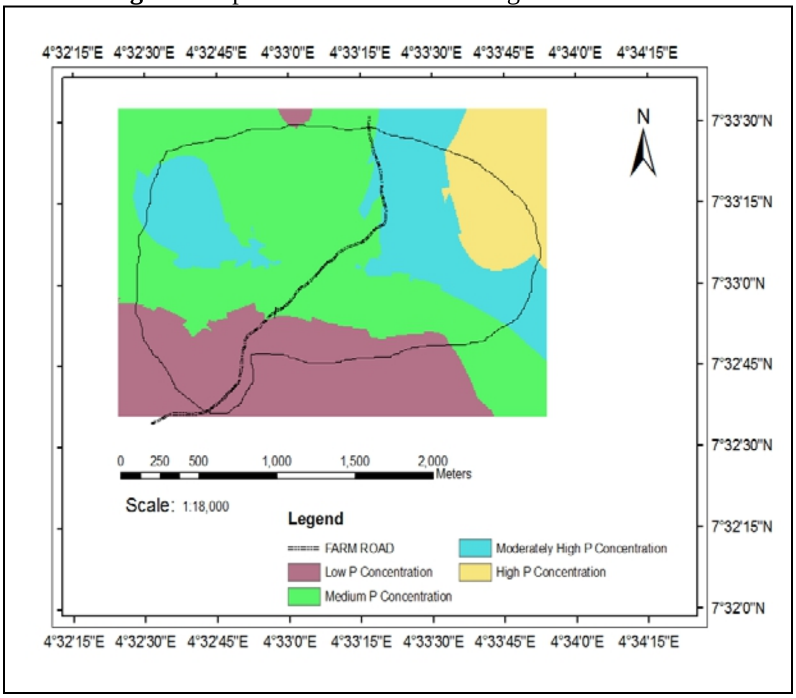

Figure 4: Spatial distribution of phosphorus concentraion

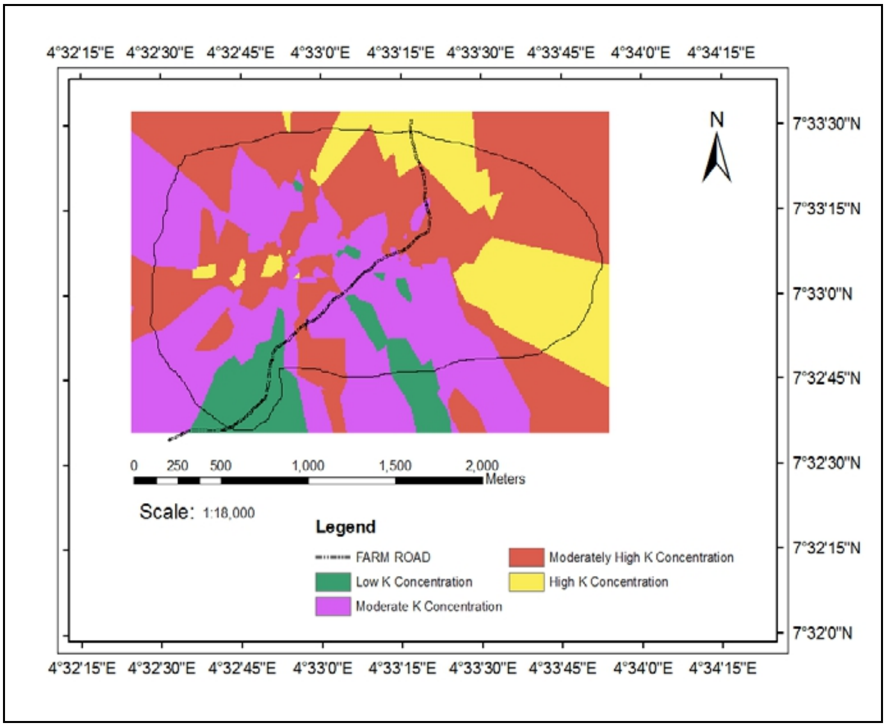

Figure 5: Spatial distribution of potassium concentraion

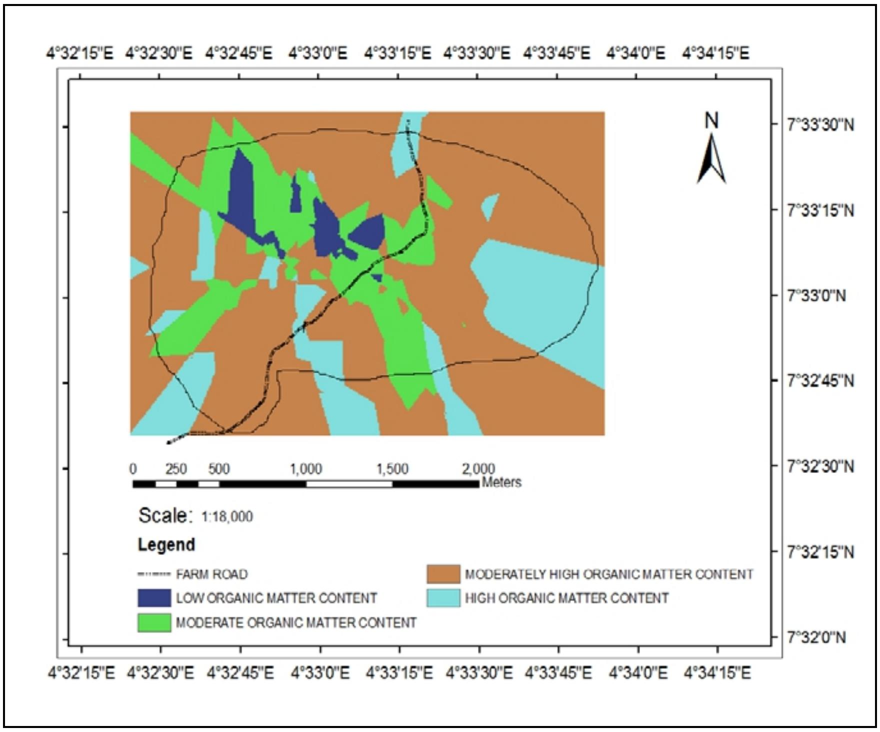

Figure 6: Spatial distribution of organic matter content

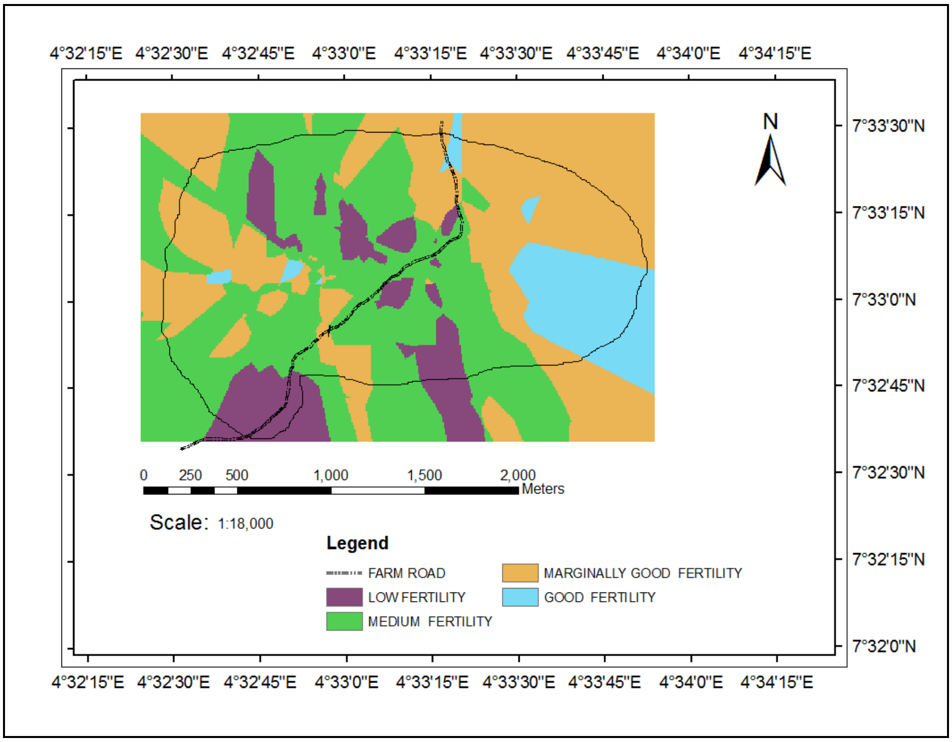

Figure 7: Fertility map of the farmland

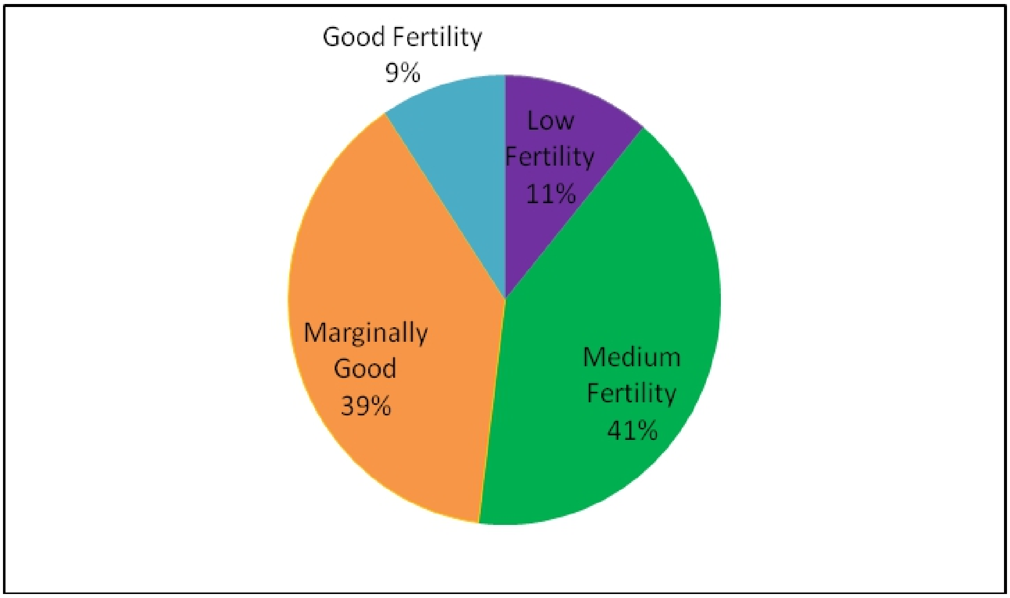

Figure 8: The percentage distribution of the fertility classes of the farmland

Discussion

The ASTER image from which the contour was generated had been previously used by researchers to generate Digital Elevation Model (DEM) of a landscape as it was applied in the DEM study of Nanggroe Aceh Darussalam Province in Indonesia (Trisakti and Carolita, 2012). The updating of the 1:50.000 topographic maps of Athens, Greece was also carried out using ASTER and Short Radar and Topographic Mission (SRTM) Digital Elevation Model (Nikolakopoulos and Chrysoulakis, 2006). Previous report had discussed the integration of satellite images with ASTER and SRTM Digital Elevation Models to produce a new data about the topographical layout of the ancient city of Ur in southern Mesopatamia (Di Giacomo and Scardozzi, 2012). ASTER had been proved to have the capability to gather data on elevation and on such other properties as the surface temperature, emissivity and reflectance of earth features and the data which could be gathered in 14 spectral bands of 3 visible and 11 on the infrared region of the electromagnetic spectrum was discussed in Gillan, (2011).

The use of the Focal Statistics Tools to improve the contour lines through removing closed contours was previously discussed in Mackaness and Steven (2006). The Focal Statistics tool indicated the neighborhood type and the statistics to be calculated in which the applications were rectangle and mean respectively. Contours had been described as lines that connected points of equal elevation value with the indication of steeper locations in areas where the contours were closer together and where there was a little change in a value, the lines were spaced further apart indicating flatter topography (Hiremath and Kodge, 2010). The output slope raster calculated as percent of slope associated lower slope value to flatter terrain and higher slope value to steeper terrain (Gokgoz, 2005). The use of slope to guide in soil sampling locations was premised on the assertion of a change of slope to depict a change in soil type (Gebrelibanos and Assen, 2013). Soils on the same slope underlain by the same rock type and parent materials had been reported to be similar as indicated in the relationship between the six main rock types identified in south west Nigeria and the corresponding soil associations (Smyth and Montgomery, 1962; Periaswamy and Ashaye, 1982). In the report , the soils of Iwo soil association, were related to the coarse grained granite and gneisses, Ondo soil association related to the medium grained granites and gneisses, Egbeda soil association related to the fine grained biotite gneisses and schists, Itagunmodi soil association related to the amphibolites, Okemessi soil association related to quartz gneisses and schists, Mamu soil association related to sericite schists

The spatial distribution of nutrient concentration of nitrogen, phosphorus, potassium and organic matter content into low, medium, moderately high and high was generated with the use of interpolation toolset, by which predicted values were assigned to all other locations to create continuous surface representation of the nutrient concentration. The kriging interpolation method used was a geostatistical method based on a statistical model of autocorrelation meant to provide some measure of the accuracy of the prediction (Royle et al., 1981; Oliver, 1990). The soil fertility map categorized into low, medium, marginally good and good fertility classes was generated by overlay operations with the use of the 3D Analyst/Raster Math/Plus Tools in ArcMap followed the previous procedures in (Liu et al., 2002). The overlay analysis was performed with the use of weighted overlay tool by which a common scale of values had been applied to the concentration of the different elements to produce an integrated soil fertility classes. The procedure corroborated the previous findings of Ebitsu and Minale (2013) in the preparation of suitability map by overlay analysis on Arc map to classify solid waste dumping in Bahir Dar Town, Ethiopia as unsuitable, moderately suitable and most suitable.

Conclusion

The slope classes of 0 to 2%, 2 to 4%, 4 to 6% and 6 to 8% generated from ASTER image formed the basis of soil sampling locations for the categorization of nutrient concentration into low, medium, moderately high and high while the soil fertility map was categorized into low, medium, marginally good and good fertility classes and with the percentage respective coverage area of 11, 41, 39 and 9% for low, medium, marginally good and good fertility classes indicating the greater percentage of the farmland to be of medium to marginally good fertility.

References:

Ben-Dor, E. and Parkin, K. Mapping of several soil properties using DAIS-7915 hyperspectra scanner data: A case study of clay soils in Israel. International Journal of Remote Sensing, Israel, 33: 1043 – 1062, 2002.

Ben-Dor, E., Chabrillat, S., Dematte, J.A.M., Taylor, R.G., Hill, J., Whiting, M.L. and Sommer, S. Using imaging Spectroscopy to study soil properties. Remote Sensing of Environment. 113: 538 – 555, 2009.

Carrow, R.N. Soil testing for fertilizer recommendation. Golf Course Management 63(11): 61 – 68, 1995.

Carter, M. R. Soil Sampling and Methods of Soil Analysis. Canadian Society of Soil Science. Lewis Publishers, London. 823pp, 1993.

Chabrillat, S., Goetz, A.F. H., Krosley, L. and Olsen, H.W. Use of Hyperspectral images in the identification and mapping of expansive clay soils and the role of spatial resolution. Remote Sensing of Environment 82: 431 – 445, . 2002.

Cook, S.E., Corner, R., Groves, P.R. and Grealish, G.J. Use of airborne gamma radiometric data for soil mapping. Australian Journal of Soil Research, 34: 183 – 194, 1996.
Di Giacomo, G. and Scardozzi, G. Multitemporal High Resolution Satellite Images for the study and Monitoring of an Ancient Mesopotamian City and its Surrounding Landscape: The Case of Ur. International Journal of Geophysics, Volume2012, Article ID716296. 14 pp, 2012.
Dinkins, C.P. Soil Sampling Strategies. MONTANA State University Extension MontGuide MT200803AG New 4/08.
http://landresources.montana.edu/soilfertility/PDFbyformat/publication%20pdfs/Soil_Sampling_Strat_MT200803AG.pdf, 2008.
Ebitsu, T.A. and Minale, A.S. Solid waste dumping site suitability analysis using geographic information system (GIS) and remote sensing for Barhir Dar Town, North Western Ethiopia. Afican Journal of Environmental Science and Technology 7(11): 976 – 989, 2013.
Franzen, D.W., Cihacek, L.J., Hofman, V.L. and Swenson, L.J. Topography-based sampling compared with grid sampling in the Northern Great Plain. Journal of Production Agriculture. 11: 364 – 370, 1998.
Gebrelibanos, T. and Assen, M. Effects of slope aspect and vegetation types on selected soil properties in a dryland Hirmi watershed and adjacent agro-ecosystem, northern highlands of Ethiopia. African Journal of Ecology. doi: 10.1111/aje.12118, 2013.
Gillan J. Advanced Space-borne Thermal Emission and Reflection Radiometer (ASTER).
http://wiki.landscapetoolbox.org/doku.php/remote_sensor_types:aster, 2011.
Gokgoz, T. Generalization of Contours Using Deviation Angles and Error Bands. The Cartographic Journal 42(2): 145 – 156, 2005.
Havlin, J.L., beaton, J.D., Tisdale, S.L. and Nelson, W.L. Soil Fertility and Fertilizers. An Introduction to Nutrient Management. Pearson Education, Inc., New Jersey, U.S.A. 515 pp, 2009.
Hiremath, P.S. and Kodge, B.G. Generating contour lines using different elevation data file formats. International Journals of Computer Science and Applications 3(1): 19 – 25, 2010.
Jarmer, T., Hill, J., Laree, H. and Sarah, P. Mapping Topsoil Organic Carbon in Non-agricultural Semi-arid and Arid Ecosystems of Israel. Photogrammetric Engineering and Remote Sensing 76(1): 85 – 94, 2010.
Jarmer, T., Vohland, M., Lilienthal, H. and Schnug, E. Estimation of some chemical properties of an agricultural soil by spectroradiometric measurements. Pedosphere, 18: 163 – 170, 2008.
Juo, A.S.R. and Franzluebbers, K. Tropical Soils. Properties and Management for Sustainable Agriculture. Oxford University Press, Oxford, U.K. 281 pp, 2003.

Kumar, N.S., Anouncia, S.M. and Pruba, M. Application of Satellite Remote Sensing to find Soil Fertilization by using Soil Colour: Study area Vellore District, Tamil Nadu, India. International Journal of Online Engineering Volume 9, No.2. online_journals.orgli-joe/article/view/2530, 2013.

Li, Z.., Huffman, T., Zhang, A., Zhou, F. and Mc Conkey, B. Spatially locating soil classes within complex soil polygons-Mapping soil capability for agriculture in Saskatchewan, Canada. Agriculture, Ecosystem and Environment, 52: 59 – 67, 2012.

Liu, W., Xia, Z. and Dai, H. A. New Approach to Assess the Positional Accuracy of Maps Generated by GIS Overlay Operations. Geospatial Information Science 5(2): 45 – 50, 2002.

Luo, Z., Yahoin, L., Jain, W. and Jing, W. Quantitative Mapping of Soil Organic Matter Material using Field Spectrometer and Hyperspectral Remote Sensing. The International Archives of the Photogrammetry, Remote Sensing and Spatial Information Sciences, Volume XXXVII Part B8. www.isprs.org/proceedings/XXXVII/congress/8.pdf/9_WG-VIII-9/09.pdf, 2008.

Mackaness, W.A. and Steven, M. An Algorithm for Localized Contour Removal over Steep Terrain. The Cartographic Journal. 43 (2): 144 – 156, 2006.

Malindo, W.A. Determination of the Nutrient Status of a Soil after Incubation with Organic Residues for Different Days in Benin City, Nigeria. World Journal of Agricultural Sciences 4(6): 731 – 736, 2008.

Mallarino, A.P. and Wittry, D.J. Efficacy of grid and zone soil sampling approaches for site specific assessment of phosphorus, potassium, pH and organic matter, Precision Agriculture 5: 131 – 144, 2004.

Nikolakopoulos, K.G. and Chrysoulakis, N. Updating the 1:50.000 topographic maps using ASTER and SRTM. DEM. The case of Athens, Greece. Remote Sensing for Environmental Monitoring, GIS Applications, and Geology and Geology VI, edited by Manfred Ehlers, Ulrich Michel, Proc. of SPIE Vol. 6366, 636606, (2006) · 0277- 786X/06/$15 · doi: 10.1117/12.689016 Proc. of SPIE Vol. 6366 636606-1, 2006.

Oliver, M.A. Kriging: A Method of Interpolation for Geographic Information Systems. International Journal of Geographic Information System 4: 313 – 332, 1990.

Periaswamy, S.P. and Ashaye, T.I. Updated Classification of some Southwestern Nigeria Soils. Ife Journal of Agriculture 4(1&2), 25 – 41, 1982.

Royle, A.G., Clausen, F.L. and Frederikksen, P. Practical Univeral Kriging and Automatic Contouring. Geoprocessing 1: 377 – 394, 1981.

Singh, B.M. and Subramanian, S.K. Use of remote sensing techniques in geomorphological and soil studies for management of irrigated areas of

Chamber Canal, Madhya Pradesh. Journal of the Indian Society Photo-Interpretation and Remote Sensing, 10(2): 67 – 73, 1982.
Smyth A.J. Montgomery, R.F. Soils and Land use in Central Western Nigeria, Ibadan Government Printer, 265pp, 1962.
Trisakti, B. and Ita Carolita, I. Comparison result of DEM generated from ASTER Stereo Data and SRTM. http://www.gisdevelopment.net/technology/tm/tm001pf.htm, 2012.
USGS, and Japan ASTER Program. ASTER scene AST_L1B_003_06262000100635, 1B, USGS, Sioux Falls, 6/26/2001. 2003, www.hindawi.com/journals/aess/2011/904561
Zribi, M., Baghdadi, N. and Nolin, M. Remote Sensing of Soil. Applied and Environment Soil Science, Volume 2011, Article ID 904561. 2pp, 2011.